NASA TECHNICAL NOTE

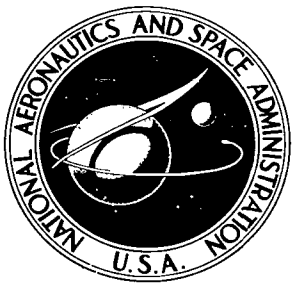

NASA TN D-7016

COMPARISON OF PREDICTED AND EXPERIMENTAL CAVITATION PERFORMANCE OF 84° HELICAL INDUCER IN WATER AND HYDROGEN

by George Kovich

Lewis Research Center

Cleveland, Ohio 44135

NATIONAL AERONAUTICS AND SPACE ADMINISTRATION • WASHINGTON, D. C. • DECEMBER 1970

1. Report No.	2. Government Accession No.	3. Recipient's Catalog No.
NASA TN D-7016		

4. Title and Subtitle	5. Report Date
COMPARISON OF PREDICTED AND EXPERIMENTAL CAVITATION PERFORMANCE OF 84° HELICAL INDUCER IN WATER AND HYDROGEN	December 1970
	6. Performing Organization Code
7. Author(s)	8. Performing Organization Report No.
George Kovich	E-5711
	10. Work Unit No.
9. Performing Organization Name and Address	128-31
Lewis Research Center National Aeronautics and Space Administration Cleveland, Ohio 44135	11. Contract or Grant No.
	13. Type of Report and Period Covered
12. Sponsoring Agency Name and Address	Technical Note
National Aeronautics and Space Administration Washington, D.C. 20546	14. Sponsoring Agency Code

15. Supplementary Notes

16. Abstract

The cavitating performance of an 84° flat-plate helical inducer was investigated in water over a range of liquid temperatures and flow coefficients. A semiempirical prediction method was used to compare predicted values of required net positive suction head in water with experimental values obtained in water and in liquid hydrogen. Good agreement between predicted and experimental data was obtained both in water and in hydrogen. The required net positive suction head in water decreased with increasing temperature and increased with flow coefficient, similar to that observed for liquid hydrogen.

17. Key Words (Suggested by Author(s))	18. Distribution Statement
Pump cavitation performance Water Liquid hydrogen Thermodynamic effects of cavitation Performance prediction	Unclassified - unlimited

19. Security Classif. (of this report)	20. Security Classif. (of this page)	21. No. of Pages	22. Price*
Unclassified	Unclassified	22	$3.00

*For sale by the National Technical Information Service, Springfield, Virginia 22151

COMPARISON OF PREDICTED AND EXPERIMENTAL CAVITATION PERFORMANCE OF 84° HELICAL INDUCER IN WATER AND HYDROGEN

by George Kovich

Lewis Research Center

SUMMARY

The cavitating performance of an 84° flat-plate helical inducer is evaluated in water at a rotative speed of 14 140 rpm. The net positive suction head (NPSH) requirements were determined over a range of water temperature from 544.7° to 814.7° R (302.6 to 452.6 K) and a flow coefficient range of 0.066 to 0.076. A semiempirical prediction method is used to compare NPSH requirements in water with those obtained for a similar inducer in liquid hydrogen. Experimental values of NPSH in water are compared with predicted values over the temperature and flow coefficient range.

Predicted values of NPSH in liquid hydrogen based on experimental data in water were in reasonably good agreement with experimental values of NPSH for a similar inducer in liquid hydrogen after adjustment for differences in measured values of NPSH between the two inducers in room-temperature water. Comparison of experimental NPSH requirements in water with predicted NPSH was good. The required NPSH in water decreased with increasing temperature and increased with increasing flow coefficient, similar to that observed for liquid hydrogen. The noncavitating performance of the inducer was unaffected by water temperature.

INTRODUCTION

Rocket engines using liquid hydrogen as fuel have pump inducers designed to operate with cavitating fluid within the blade passages. This permits pump operation at lower values of inlet net positive suction head (NPSH), and hence lower fuel tank pressures are possible. This is advantageous for tank construction and overall vehicle weight. A substantial portion of inlet pressure reduction obtained when operating with

inducer cavitation is due to the thermodynamic properties of liquid hydrogen. It was shown in references 1 to 3 that the required net positive suction head for a given operating condition with cavitation changed with hydrogen temperature. This change in required NPSH is attributed to localized cooling of the fluid by vaporization during cavitation and is referred to as the thermodynamic effect of cavitation. The vaporization process also results in a lower cavity pressure. A detailed description of the cavitation process in a venturi, together with experimental data relating the amount of thermodynamic effects of cavitation to pressure changes within the vapor cavity, is presented in references 4 and 5. The change in thermodynamic effects of cavitation with temperature is equated to the change in venturi inlet pressure required to maintain a constant cavity size for a given flow condition. A semiempirical relation was developed from the venturi investigations to predict the magnitude of the thermodynamic effects of cavitation. This prediction method was extended to inducers and pumps in reference 6.

Water exhibits essentially no thermodynamic effects of cavitation at room temperature. However, at higher temperatures (greater than approximately 660° R or 367 K) the thermodynamic effects of cavitation for water become significant. For example, the thermodynamic effects of cavitation for water at 734.7° R (408.2 K) are about the same as those for liquid hydrogen at 28° R (15.6 K)(ref. 6). The use of water in place of liquid hydrogen in experimental research and for development tests of rocket engine inducers and pumps offers considerable potential savings in facility and operating costs. Operating hazards would also be minimized. It is therefore desirable to evaluate the relation of the performance of a cavitating inducer in high-temperature water with that obtained in liquid hydrogen.

The purpose of this investigation is to evaluate the feasibility of testing in high-temperature water to simulate the cavitating performance of an inducer in liquid hydrogen. In the present study the cavitation performance of an 84° flat-plate helical inducer was evaluated in high-temperature water. The required NPSH in water was determined for a range of flow coefficients from 0.066 to 0.076 at water temperatures from 544.7° to 814.7° R (302.6 to 452.6 K). Rotative speed was 14 140 and 10 000 rpm. The required NPSH in water is compared with that obtained in hydrogen for a similar inducer (ref. 7). Water data were converted to equivalent hydrogen data with the prediction method of reference 6. The investigation was conducted at the Lewis Research Center.

APPARATUS AND PROCEDURE

Test Inducer

The test inducer used in the water investigation was a stainless-steel three-bladed flat-plate helical inducer with a tip helix angle of 84°. This inducer and details of its

geometry are shown in figure 1. The aluminum inducer tested in hydrogen was of identical geometric design. A photograph and geometric details of that inducer are presented in reference 7. The blade leading edges of each inducer were faired on the suction surface only.

Test Facility

This investigation was conducted using the Lewis high-temperature water tunnel, a vertical closed-loop pump test facility. A schematic of the loop is shown in figure 2 and the facility is depicted in figure 3. A detailed description of the facility is given in reference 8.

For test operations the loop is filled with demineralized water. The gas content of the water is then reduced to less than 3 ppm by weight in an auxiliary degasifier system. Particles 5 micrometers or larger are removed by filtering during the degasifying process. The water is heated to the desired temperature by the gas-fired crossflow heat exchanger in the bypass leg paralleling the flow control valve.

Instrumentation and Procedure

Pressure and temperature instrumentation to measure overall performance of the inducer was located in the pump inlet line approximately 36 inches (91.4 cm) ahead of the rotor leading edge and at the inducer discharge, 1 inch (2.5 cm) downstream of the rotor trailing edge. Inducer inlet water temperature was measured with a calibrated closed-end copper-constantan thermocouple located in the center of the flow stream at the inlet measuring station. Inlet static pressure was obtained with four pipe-wall taps at the inlet station. One shielded total-pressure probe at mid-blade height was located at the outlet measuring station. All pressures were measured with calibrated strain-gage pressure transducers. Flow rate was measured by a venturi flowmeter. Rotative speed was measured with a frequency counter in conjunction with a magnetic pickup. All data were recorded by an automatic digital potentiometer.

The estimated measurement errors due to instrumentation are presented in the following table for the upper and lower limits of water temperature: The errors were assumed to vary linearly between the upper and lower temperature limits.

Parameter	Water temperature limit	
	544.7° R (302.6 K)	814.7° R (452.6 K)
	Error	
Inlet total head, ft (m)	±0.5 (±0.2)	±2 (±0.6)
Net positive suction head, ft (m)	±0.5 (±0.2)	±5 (±1.5)
Head rise across inducer, ft (m)	±1 (±0.3)	±1 (±0.3)
Venturi flow, percent	±0.5	±0.5
Rotor speed, rpm	±30	±30
Temperature, °R (K)	±0.5 (±0.28)	±0.5 (±0.28)

Water tests were conducted at the rotative speed of 14 140 rpm. Cavitation performance at three flow coefficients (φ = 0.066, 0.072, and 0.076) was determined at each of four nominal water temperatures. Cavitating performance was obtained by maintaining a constant flow while reducing the inducer inlet pressure. Inducer inlet pressure (net positive suction pressure) was decreased until the inducer head-rise coefficient had deteriorated to at least 70 percent of the noncavitating head-rise coefficient value. The noncavitating head-rise coefficient was obtained at a sufficiently high value of inducer inlet pressure to ensure that cavitation had no effect on the inducer performance. Vapor pressure of the water was based on the inducer inlet water temperature. The net positive suction pressure was obtained as the difference between inducer inlet total pressure and the inlet water vapor pressure.

The cavitation performance of both inducers, the water inducer model and the aluminum inducer model tested in hydrogen, was determined over the range of flow coefficients at a rotative speed of 10 000 rpm in room-temperature water.

RESULTS AND DISCUSSION

Noncavitating Performance

The noncavitating performance of the inducer is defined as that which shows no measurable change in inducer head rise when the net positive suction head (NPSH) is either increased or decreased. The noncavitating head-rise coefficient ψ_{nc} for the water model inducer is plotted as a function of flow coefficient φ in figure 4 for several water temperatures at a NPSH of approximately 200 feet (61.0 m). As expected, no effect of water temperature on the noncavitating inducer performance was observed. These noncavitating values of head-rise coefficient will be used to obtain the ratio of cavitating to noncavitating head-rise coefficient ψ/ψ_{nc} for later presentation of the inducer cavitation data.

Cavitation Performance

The cavitating to noncavitating head-rise coefficient ratio ψ/ψ_{nc} for the water model inducer is plotted as a function of NPSH in figure 5 for three nominal values of φ (0.076, 0.072, and 0.066) and several water temperatures. The gradual drop in the value of ψ/ψ_{nc} before the final falloff in performance because of cavitation is characteristic of this inducer. The sharp dips in performance observed before the final falloff in performance represent areas of unstable operation in the inducer. As in reference 7, a value of 0.70 for ψ/ψ_{nc} was arbitrarily chosen to compare performance in subsequent analyses.

The values of NPSH that correspond to the fluid velocity head $V_1^2/2g$ at the inducer inlet for each value of φ are shown as vertical dashed lines in figure 5. At this condition the local static pressure at the inducer inlet equals the vapor pressure and thus any further reduction in the NPSH causes boiling in the inlet line, with the resulting vapor being ingested by the inducer.

As the water temperature is increased, the required NPSH decreases for a constant value of ψ/ψ_{nc}. Some decrease in required NPSH also occurs as the value of ψ/ψ_{nc} is decreased for each value of φ and each temperature.

The required NPSH for a ψ/ψ_{nc} of 0.70 is shown as a function of φ at the various nominal water temperatures in figure 6. The required NPSH increases with increased φ-values and decreases with increased water temperature. Except at 814.7° R (452.6 K), the effect of temperature on required NPSH is generally greater as the flow coefficient is decreased. At 814.7° R (452.6 K) and the lower flow coefficients, the inducer performance starts to be influenced by vapor in the inlet line when the required NPSH-value approaches the inlet line velocity head $V_1^2/2g$. The shaded portion of figure 6 represents a condition of vapor in the inducer inlet. The flattening of the 814.7° R (452.6 K) curve at the low φ-values probably occurs initially as a result of localized cavitation occurring on the inlet hub strut supports as the local static pressure becomes equal to the vapor pressure of the water. These trends with temperature and flow coefficient compare favorably with those observed for a similar inducer in liquid hydrogen (see fig. 6 in ref. 7).

Prediction Method for Thermodynamic Effects of Cavitation

Before predicted and experimental cavitation results are compared, a brief review of a prediction method for thermodynamic effects of cavitation and its application to pumps is presented.

Venturi cavitation studies (refs. 4 and 5) have shown that with flow similarity, that is, a given flow velocity and cavity size, a reduction in cavity pressure allows a corresponding reduction in the inlet pressure requirements (NPSH for a pump). For a given pump, it can be assumed that the cavity size or vapor volume is the same at a given head-rise coefficient ratio ψ/ψ_{nc} and flow coefficient for various fluids. The experimental studies of references 2 and 6 tend to verify this assumption.

While direct measurement of the cavity pressure in a pump is not feasible, the cavity pressure depression at the given head-rise coefficient ratio and flow coefficient of interest can be estimated by observing changes in required NPSH with changes in fluid temperature, fluids, and/or rotative speed. (A reduction in cavity pressure allows a corresponding reduction in the NPSH.) The method for estimating cavity depressions is described in detail in reference 6. Equations pertinent to the procedure are presented below.

Values of cavity pressure depression below vapor pressure Δh_v corresponding to a free-stream temperature can be closely estimated for a fluid by the equation (ref. 6)

$$\Delta h_v = \frac{L}{C_p} \frac{\rho_v}{\rho_l} \left(\frac{dH_{vp}}{dT} \right) \frac{\gamma_v}{\gamma_l} \tag{1}$$

The known properties of a fluid are used to obtain values of Δh_v as a function of the vapor- to liquid-volume ratio γ_v/γ_l. To account for fluid property changes as the temperature is reduced by vaporization, equation (1) may be solved by numerical integration. The values of vapor pressure depression Δh_v are plotted as a function of vapor- to liquid-volume ratio γ_v/γ_l for a range of temperatures for water in figure 7 and for hydrogen in figure 8. The curves essentially reflect the thermodynamic properties of each fluid (eq. (1)) and are constructed primarily for use in the prediction method; however, it is interesting that the Δh_v-values obtained for hydrogen in the range of temperature from 24.9° to 35.0° R (13.8 to 19.4 K) are comparable with those for water from room temperature to 859.7° R (477.6 K).

The absolute value of γ_v/γ_l for a particular pump cannot be experimentally determined. However, it is shown in reference 6 that a reference value of γ_v/γ_l can be established experimentally for a particular pump by the determination of the cavity pressure depression Δh_v. Two sets of experimental data are required to establish the reference γ_v/γ_l for each desired value of head-rise coefficient ratio and flow coefficient. These data need not be for the same liquid, liquid temperature, or pump rotative speed; however, at least one of these must yield measurable thermodynamic effects of cavitation. Values of γ_v/γ_l for the desired conditions of interest can then be estimated with respect to the reference value of γ_v/γ_l from the following equation (ref. 6):

$$\frac{\gamma_v}{\gamma_l} = \left(\frac{\gamma_v}{\gamma_l}\right)_{ref} \left(\frac{\alpha_{ref}}{\alpha}\right)\left(\frac{N}{N_{ref}}\right)^{0.8} \tag{2}$$

Values of Δh_v corresponding to the γ_v/γ_l for the conditions of interest can be used with the following equation to predict the required NPSH for a particular pump operated with cavitation at a fixed flow coefficient and head-rise coefficient ratio but with changes in liquid, liquid temperature, and/or rotative speed:

$$\frac{(NPSH)_{ref} + (\Delta h_v)_{ref}}{NPSH + \Delta h_v} = \left(\frac{N_{ref}}{N}\right)^2 \tag{3}$$

For a fixed rotative speed, equation (3) reduces to

$$(NPSH)_{ref} - NPSH = \Delta h_v - (\Delta h_v)_{ref} \tag{4}$$

which states that a change in NPSH requirements for different liquids and/or liquid temperatures is equal to the change in the pressure depression Δh_v within the cavitated region. A detailed description of the procedure for predicting NPSH requirements for conditions of interest for a particular pump is presented in reference 6.

Comparison of Predicted and Experimental Performance in Water

The required NPSH values at nominal water temperatures of 715.7° and 763.7° R (397.6 and 424.3 K) from figure 6 were used in equation (4) to obtain a value for $\Delta h_v - (\Delta h_v)_{ref}$ at a given flow coefficient. The data at 763.7° R (397.6 K) were arbitrarily chosen as the reference. A reference value of γ_v/γ_l was established for each flow coefficient by the technique described in reference 6. This reference value of γ_v/γ_l was then used with equations (2) and (4) and figure 7 to obtain NPSH requirements at other water temperatures for each particular φ-value.

A comparison between predicted and experimental values of required NPSH as a function of flow coefficient φ is presented in figure 9 for the water model inducer in water at a ψ/ψ_{nc}-value of 0.70 for various temperatures. The predicted and experimental values of NPSH for water compare reasonable well above the region where vapor is formed in the inlet line. The accuracy of the predicted curve for the water temperature of 544.7° R (302.6 K) is highly dependent upon experimental accuracy of measured NPSH at the reference temperature. Thus agreement between predicted and experimen-

tal NPSH at 544.7° R (302.6 K) is considered within experimental accuracy. The comparison of the predicted and experimental values of NPSH at 814.7° R (452.6 K) for the lower flow coefficients indicates that the predicted values of NPSH may not be reliable where the required NPSH is close to or equal to the inducer inlet velocity head. This is due to probable localized cavitation, previously mentioned, which preceeds general boiling in the inlet line. Values of NPSH less than the inducer inlet velocity head $V_1^2/2g$ are again indicated by the shaded area. Predicted values of NPSH are not shown for this region because the prediction method of reference 6 is based on similarity of cavitating flow within the blade passages. This similarity of flow is not maintained when vapor or boiling is present in the inlet line.

Prediction of Performance in Hydrogen from Measured Performance in Water

Predicted values of NPSH were determined for the water model inducer in liquid hydrogen at a rotative speed of 20 000 rpm from the performance results in water. Equations (2) and (3) and figure 8 were used, together with the reference values of γ_v/γ_l previously determined at the arbitrary reference water temperature of 763.7° R (424.3 K), to obtain predicted values of NPSH in hydrogen. The predicted values of NPSH for the water model inducer in liquid hydrogen were then compared in figure 10 with measured NPSH-values for a similar inducer tested in liquid hydrogen (ref. 7). Although similar trends were observed, a difference of 10 to 20 feet (3.0 to 6.0 m) between predicted and experimental values of NPSH was observed over most of the temperature range in hydrogen.

The differences observed indicate that the initial assumption of similarity of cavitated regions in the two inducers based on the similarity of geometric design might not be valid. A comparison of the cavitation performance for the two inducers on the basis of required NPSH as a function of flow coefficient, could qualitatively establish this similarity for conditions where no thermodynamic effects of cavitation exist, for example, for room-temperature water or for hydrogen at its triple point. Agreement between the resulting two curves would imply that the vapor cavity volumes were essentially the same for corresponding flow coefficients since the inducers are of identical geometric design.

A comparison of the required NPSH for the two inducers in room-temperature water is shown in figure 11. The required NPSH as a function of flow coefficient is presented for a ψ/ψ_{nc} of 0.70. The aluminum model of the inducer tested in hydrogen was held to a rotative speed of 10 000 rpm because of stress limitations in water. Blade leading-edge damage at the tips occurred during the cavitation performance run of the hydrogen

model inducer at the lower nominal flow coefficient of 0.066. The results show a measurable difference in the values of measured NPSH, about 2.5 feet (0.8 m), over the range of flow coefficients at this rotative speed of 10 000 rpm. This indicates that some difference in vapor cavity volume must exist for the two inducers at a fixed flow coefficient. The predicted values of NPSH for hydrogen based on the cavitation performance of the water model inducer can therefore be expected to be lower than the measured values for the hydrogen model inducer by an amount equal to or greater than this difference in measured NPSH. For example, the 2.5-foot (0.8-m) difference in the NPSH curves at 10 000 rpm will result in a difference of at least 10 feet (3.0 m) at the comparison speed of 20 000 rpm. Because hydrogen at its triple point, 24.9° R (13.8 K), has no thermodynamic effects of cavitation, equation (3) was used to predict the hydrogen performance (NPSH) for the hydrogen model inducer at 20 000 rpm and 24.9° R (13.8 K) (upper curve of fig. 11) from the results obtained at 10 000 rpm in room-temperature water. Assuming the differences in thermodynamic effects of cavitation for the two inducers to be small, the Δh_v-values calculated for hydrogen from the high-temperature-water data were then subtracted from the 24.9° R (13.8 K) curve to obtain the predicted values of NPSH at the higher hydrogen temperatures. A comparison of predicted and experimental NPSH in hydrogen for the hydrogen model inducer, determined by this procedure, is shown in figure 12. In contrast to predicted results based on water model inducer data alone (fig. 10) the limited experimental data available for liquid hydrogen now show reasonably good agreement with predicted cavitation performance at temperatures of 27.9° and 30.9° R (15.7 and 17.4 K).

The difference between experimental and predicted values of NPSH at 34° R (19.1 K) may be, in part, the result of the difference in vapor cavity volumes as indicated by the difference in NPSH in room-temperature water for the two inducers. The differences in thermodynamic effects of cavitation (vapor cavity volumes) for the two inducers would increase in magnitude at the higher hydrogen temperatures. Effects of experimental error on the predicted values of NPSH also increase with increased fluid temperature. If, for example, the measured value of $NPSH_1 - NPSH_2$ for the reference water temperatures of 715.7° and 763.7° R (397.6 and 424.3 K) and flow coefficient 0.76 is altered by only 0.5 foot (0.15 m), the corresponding changes in predicted NPSH for liquid hydrogen are 0.7 and 6.0 feet (0.23 and 1.96 m) at temperatures of 27.9° and 34° R (15.5 and 18.9 K), respectively.

CONCLUDING REMARKS

The results of this investigation demonstrate that the cavitation performance of an inducer in liquid hydrogen can be predicted with a reasonable degree of accuracy from

the cavitation performance measured in high-temperature water. Significant errors in predicted performance at the higher hydrogen temperatures, however, can occur as a result of small errors in measured performance for water.

Care should be exercised when using more than one inducer model of the same geometric design in an experimental program in which the predicted cavitation performance of one is compared with experimental results of the other. The vapor cavity volume on the blade surface is sensitive to small differences in leading-edge geometry, blade fairing, and surface roughness. These small differences resulting from machining tolerances in manufacture can effect variations in cavitation performance between inducer models of the same geometric design. These variations in NPSH may be expected to become larger as the inducer rotative speeds increase. The prediction method herein applied to pumps depends on geometric similarity of the cavitated region in the blade passages. Thus some verification of the geometric similarity of cavitation between inducer models of the same geometric design should be made, other than assumption based strictly on comparison of physical dimensions.

Inducers designed for operation in liquid hydrogen are usually stress-limited to a lower rotor speed when operated in water because of the larger hydrodynamic loading. Scaling the size of the inducer will allow operation in water at rotative speeds approaching the design speeds in liquid hydrogen. The scope of this investigation was not sufficient to define practical limits of dimensional scaling or the maximum difference between reference and predicted rotative speeds for reliable application of the prediction method.

SUMMARY OF RESULTS

The cavitation performance for an 84° flat-plate helical inducer was measured in water at temperatures from 544.7° to 814.7° R (302.6 to 452.6 K). The flow coefficient range was 0.066 to 0.076 at a rotor speed of 14 140 rpm. The cavitation performance in liquid hydrogen is predicted from the water data with an available semiempirical prediction method. The values of NPSH in liquid hydrogen predicted from water results are compared with the measured NPSH-values for a similar inducer in liquid hydrogen at temperatures from 27.9° to 34° R (15.5 to 18.9 K) for a rotative speed of 20 000 rpm.

1. The predicted values of NPSH in liquid hydrogen, based on experimental data in water, were in good agreement with experimental values of NPSH in liquid hydrogen after adjustment was made for a measured difference in cavitation performance between the two inducers in room-temperature water.

2. The predicted and experimental values of NPSH in high-temperature water were in good agreement.

3. The required NPSH in high-temperature water decreased with increasing temperature and increased with flow coefficient, similar to that observed for liquid hydrogen.

4. The noncavitating performance of the inducer is independent of water temperature.

Lewis Research Center,
National Aeronautics and Space Administration,
Cleveland, Ohio, September 21, 1970,
128-31.

APPENDIX - SYMBOLS

C_p	specific heat of liquid, Btu/(lbm)(^oR); J/(kg)(K)
g	local acceleration due to gravity, 32.163 ft/sec^2; 9.80 m/sec^2
H_{vp}	vapor pressure head, ft; m
Δh_v	cavity pressure drop below vapor pressure, ft; m
L	latent heat of vaporization, Btu/lbm; J/kg
N	rotational speed, rpm
NPSH	net positive suction head, ft; m
T	temperature, ^oF; K
V_1	inlet velocity, ft/sec; m/sec
γ_v/γ_l	vapor-volume to liquid-volume ratio
α	thermal diffusivity, ft^2/hr; m^2/hr
ρ_l	liquid density, lbm/cu ft; kg/cu m
ρ_v	vapor density, lbm/cu ft; kg/cu m
φ	flow coefficient
ψ	head-rise coefficient
ψ_{nc}	noncavitating head-rise coefficient
ψ/ψ_{nc}	ratio of cavitating to noncavitating head-rise coefficient

REFERENCES

1. Ball, Calvin L.; Meng, Phillip R.; and Reid, Lonnie: Cavitation Performance of 84° Helical Pump Inducer Operated in 37° and 42° R Liquid Hydrogen. NASA TM X-1360, 1967.

2. Ruggeri, Robert S.; Moore, Royce D.; and Gelder, Thomas F.: Method for Predicting Pump Cavitation Performance. Paper presented at the Ninth Liquid Propulsion Symposium, Interagency Chemical Rocket Propulsion Group, St. Louis, Oct. 25-27, 1967.

3. Wilcox, Ward W.; Meng, Phillip R.; and Davis, Roger L.: Performance of an Inducer-Impeller Combination at or near Boiling Conditions for Liquid Hydrogen. Advances in Cryogenic Engineering. Vol. 8. K. D. Timmerhaus, ed., Plenum Press, 1963, pp. 446-455.

4. Gelder, Thomas F.; Ruggeri, Robert S.; and Moore, Royce D.: Cavitation Similarity Considerations Based on Measured Pressure and Temperature Depressions in Cavitated Regions of Freon 114. NASA TN D-3509, 1966.

5. Moore, Royce D.; and Ruggeri, Robert S.: Prediction of Thermodynamic Effects of Developed Cavitation Based on Liquid-Hydrogen and Freon-114 Data in Scaled Venturis. NASA TN D-4899, 1968.

6. Ruggeri, Robert S.; and Moore, Royce D.: Method for Prediction of Pump Cavitation Performance for Various Liquids, Liquid Temperatures, and Rotative Speeds. NASA TN D-5292, 1969.

7. Meng, Phillip R.: Change in Inducer Net Positive Suction Head Requirement with Flow Coefficient in Low Temperature Hydrogen (27.9° to 36.6° R). NASA TN D-4423, 1968.

8. Cunnan, Walter S.; Kovich, George; and Reemsnyder, Dean C.: Effect of Fluid Temperature on the Cavitation Performance of a High Hub-Tip Ratio Axial Flow Pump in Water to 250° F (394 K). NASA TN D-5318, 1969.

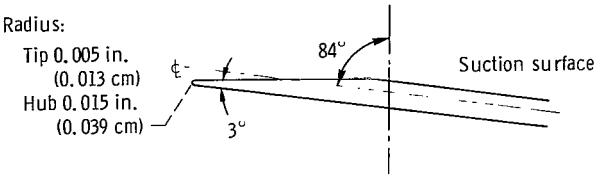

Tip helix angle (from axial direction), deg	84
Rotor tip diameter, in. (cm)	4.976 (12.639)
Rotor hub diameter, in. (cm)	2.478 (6.294)
Hub-tip ratio	0.498
Number of blades	3
Axial length, in. (cm)	2.00 (5.08)
Peripheral extent of blades, deg	440
Tip chord length, in. (cm)	19.14 (48.62)
Hub chord length, in. (cm)	9.51 (24.16)
Solidity	3.838
Tip blade thickness, in. (cm)	0.067 (0.170)
Hub blade thickness, in. (cm)	0.100 (0.254)
Radial tip clearance, in. (cm)	0.025 (0.064)
Ratio of tip clearance to blade height	0.020

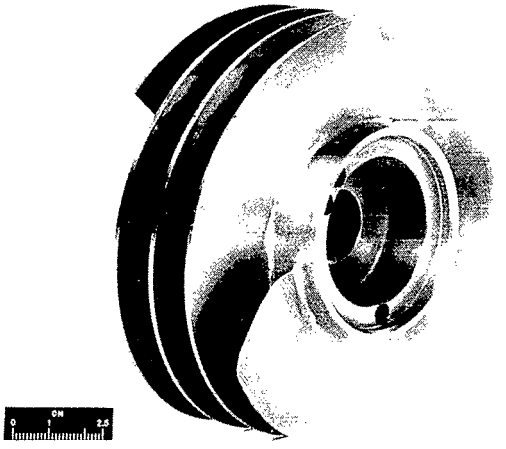

Figure 1. - 84° Helical inducer, showing geometric details.

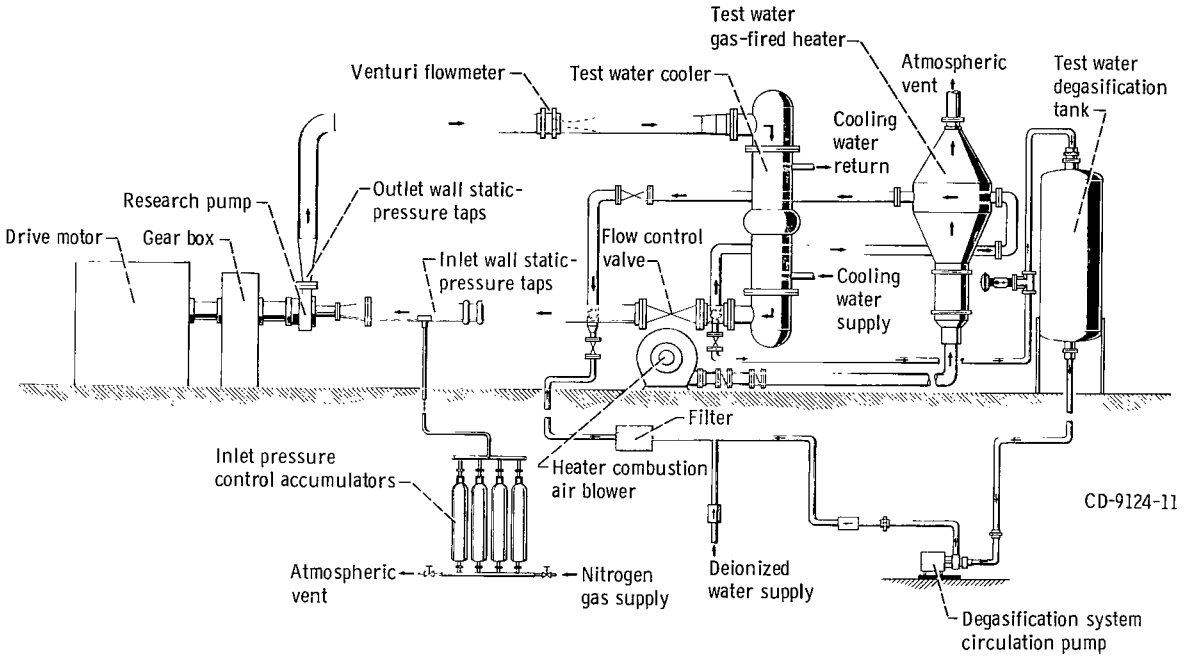

Figure 2. - Schematic of high-temperature water tunnel.

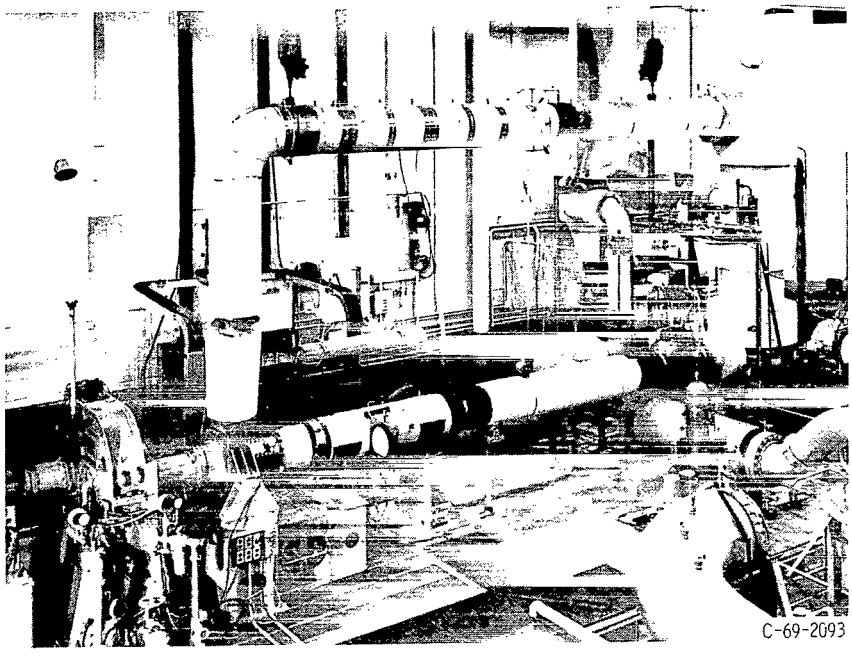

Figure 3. - High-temperature water tunnel.

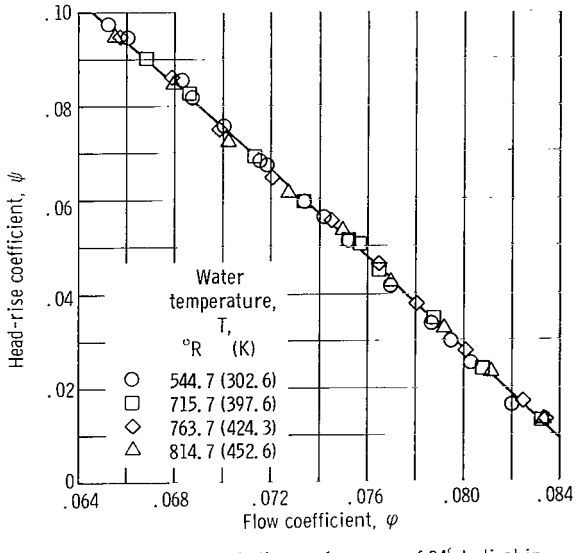

Figure 4. - Noncavitating performance of 84° helical inducer in water at rotative speed of 14 140 rpm.

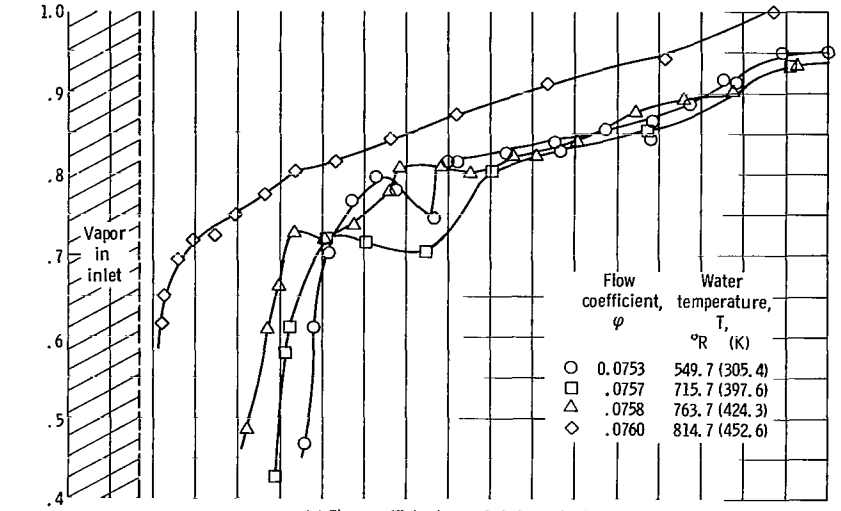

(a) Flow coefficient, φ = 0.076 nominal.

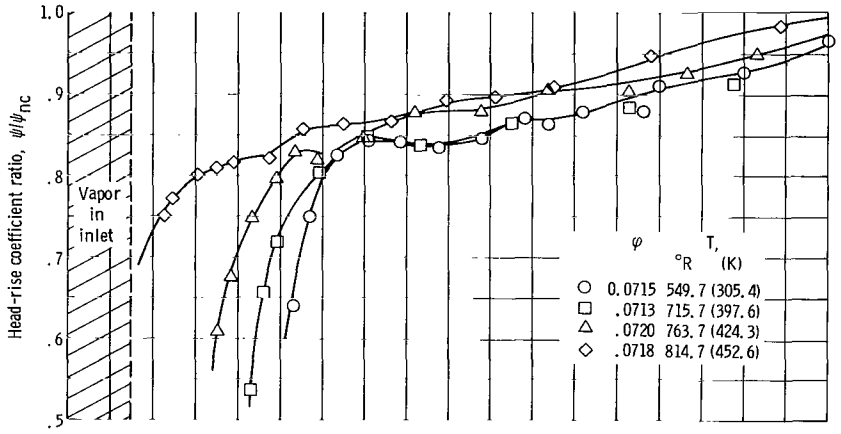

(b) Flow coefficient, φ = 0.072 nominal.

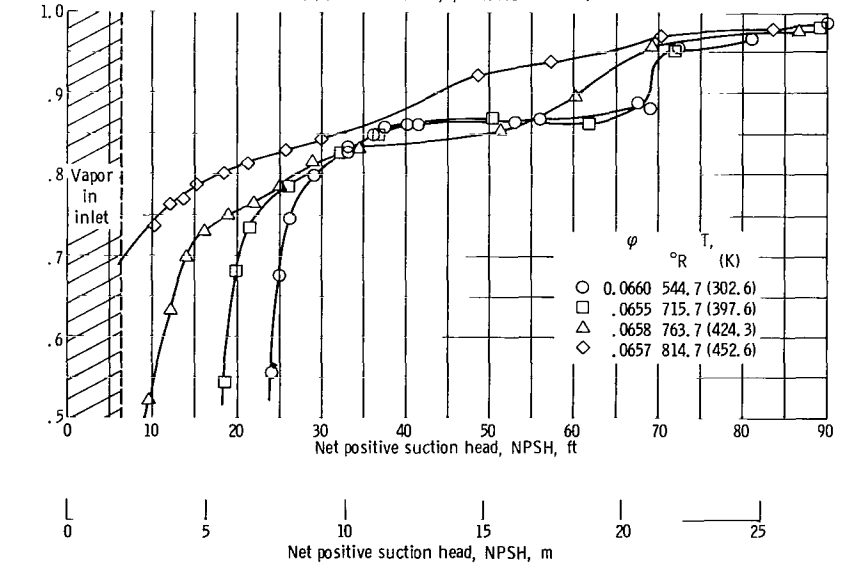

(c) Flow coefficient, φ = 0.066 nominal.

Figure 5. - Cavitating performance of 84° helical inducer in water at rotative speed of 14 140 rpm.

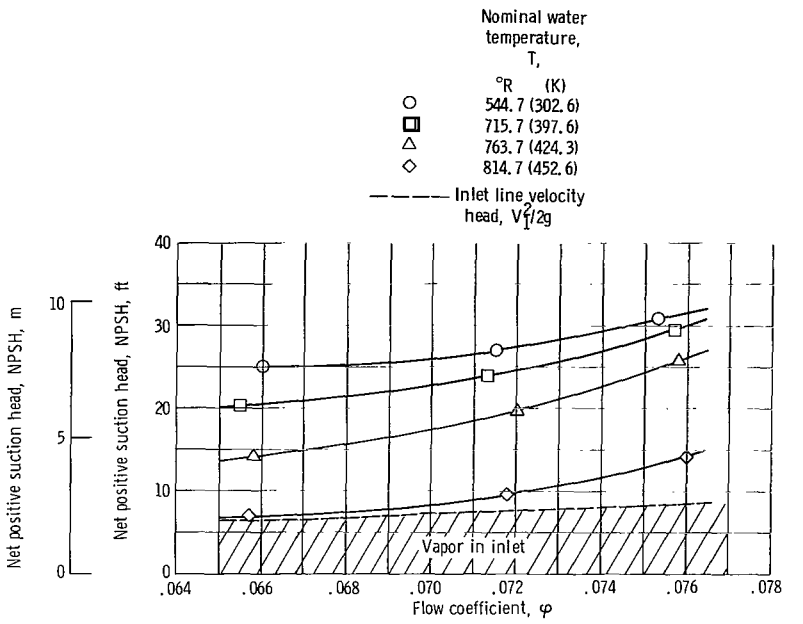

Figure 6. - Variation of net positive suction head with flow coefficient for 84° helical inducer in water at rotative speed of 14 140 rpm. Ratio of cavitating to noncavitating head-rise coefficient, $\psi/\psi_{nc} = 0.70$.

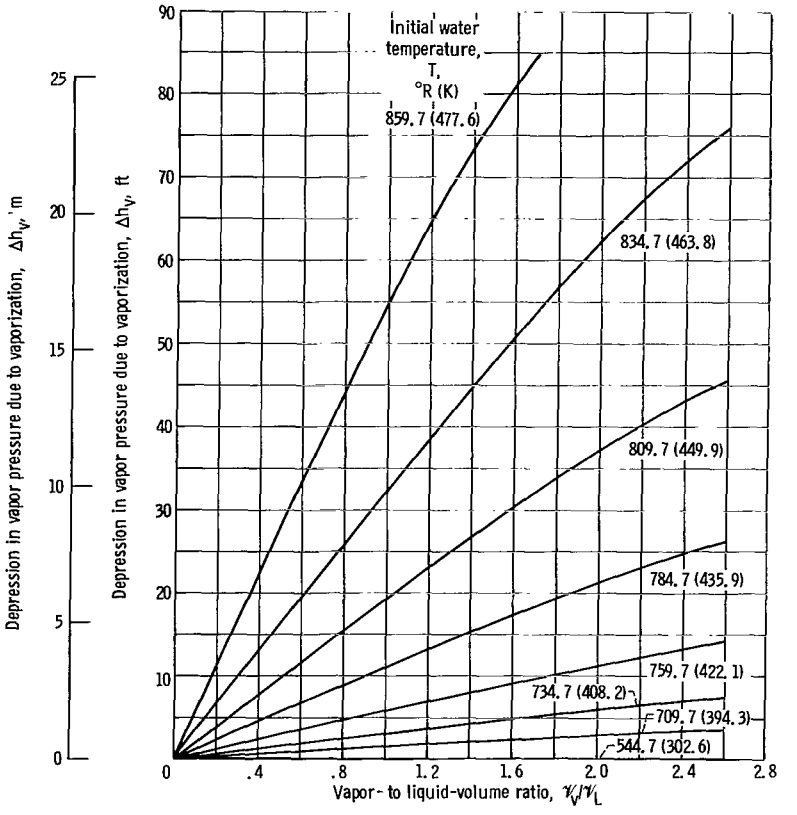

Figure 7. - Calculated vapor pressure depression due to vaporization as a function of liquid water temperatures.

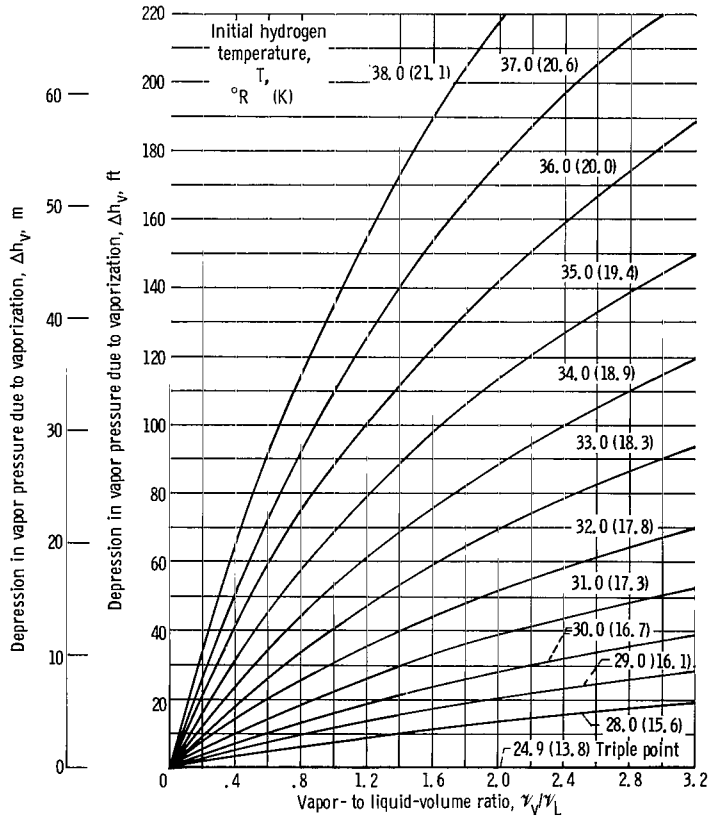

Figure 8. - Calculated vapor pressure depression due to vaporization as function of liquid hydrogen temperatures.

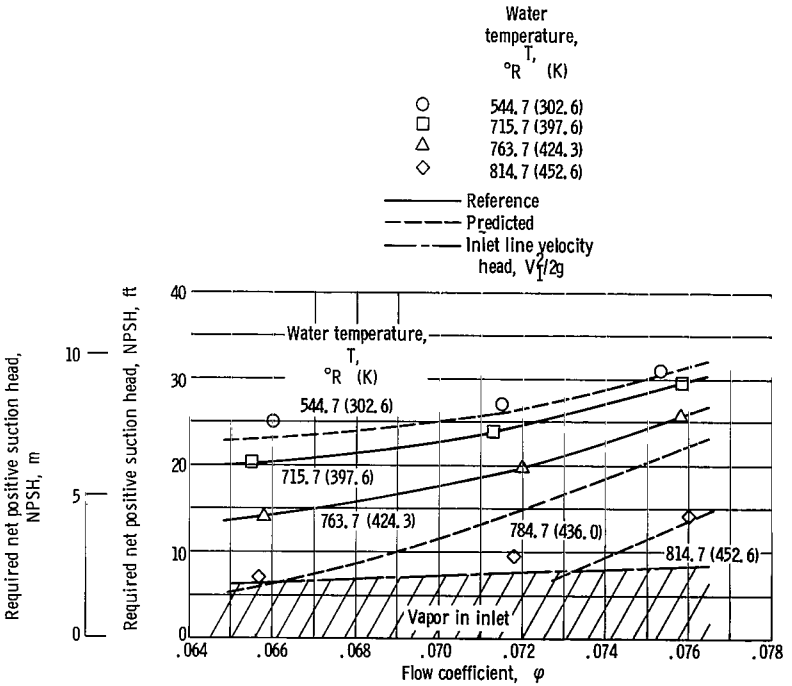

Figure 9. - Comparison of predicted and experimental values of required net positive suction head for 84° water model inducer in water. Rotative speed, 14 140 rpm; head-rise coefficient ratio, $\psi/\psi_{nc} = 0.70$.

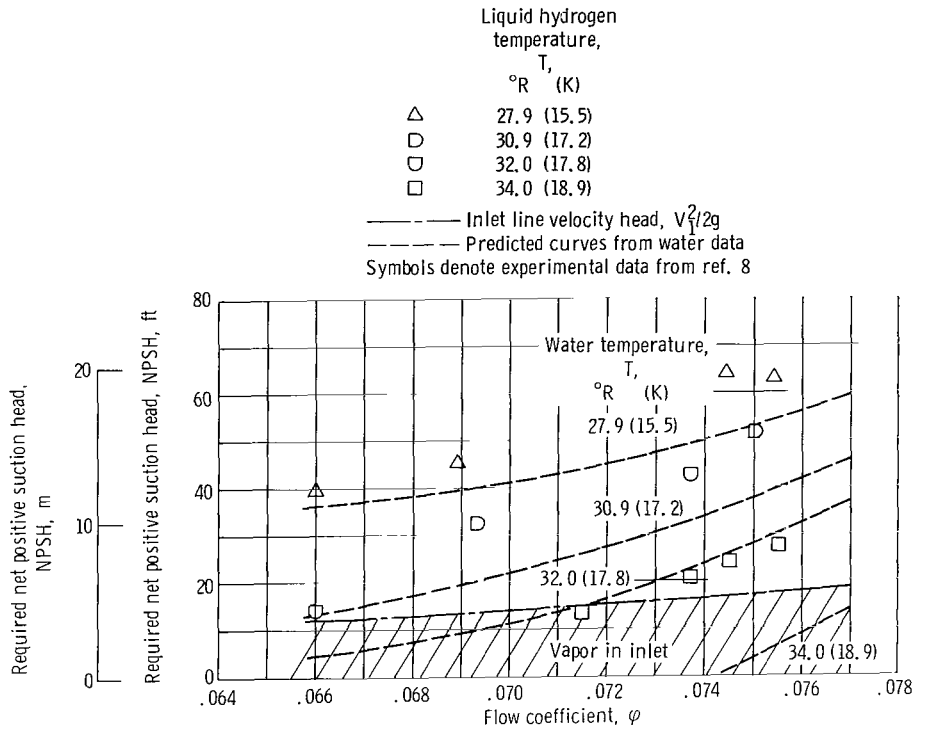

Figure 10. - Comparison of predicted and experimental values of required net positive suction head for 84° water model inducer in hydrogen. Rotative speed, 20 000 rpm; head-rise coefficient ratio, $\psi/\psi_{nc} = 0.70$.

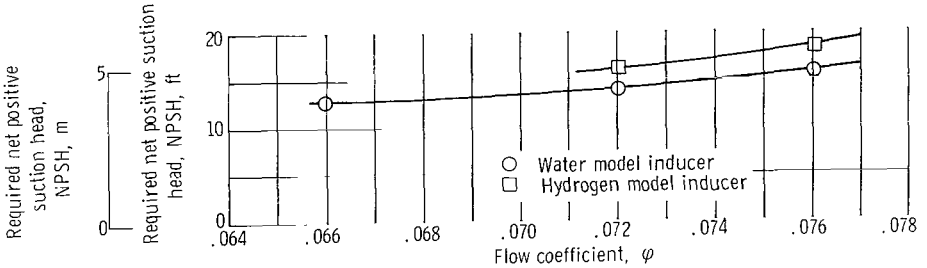

Figure 11. - Comparison of required net positive suction head in water for two 84° inducers. Rotative speed, 10 000 rpm, head-rise coefficient ratio, $\psi/\psi_{nc} = 0.70$; nominal water temperature, 544.7° R (302.6 K).

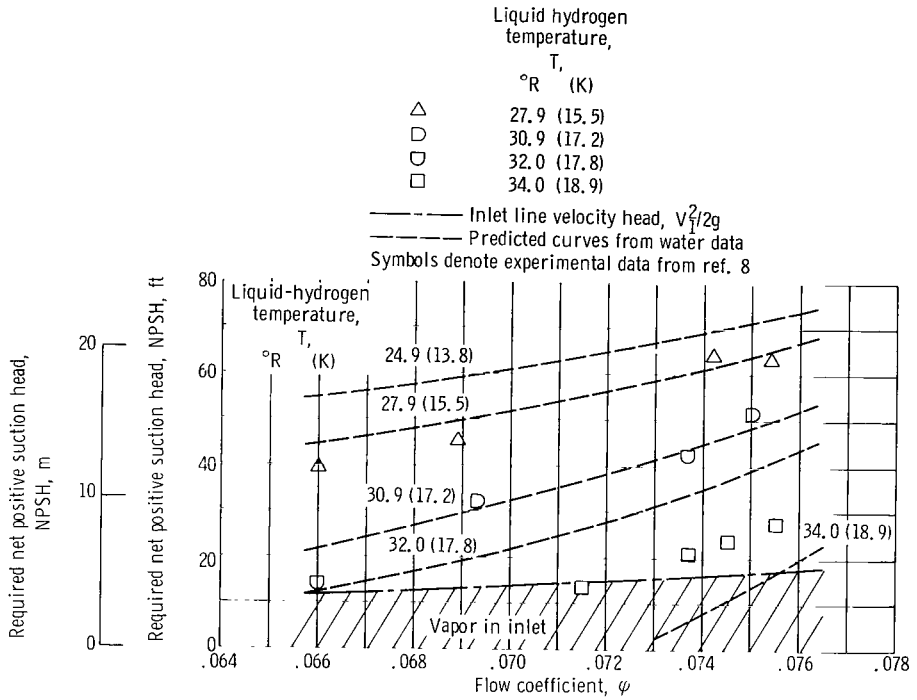

Figure 12. - Comparison of predicted and measured values of required net positive suction head for 84 hydrogen model inducer in hydrogen based on water data. Rotative speed, 20 000 rpm; head-rise coefficient ratio, $\psi/\psi_{nc} = 0.70$.

"The aeronautical and space activities of the United States shall be conducted so as to contribute . . . to the expansion of human knowledge of phenomena in the atmosphere and space. The Administration shall provide for the widest practicable and appropriate dissemination of information concerning its activities and the results thereof."

—NATIONAL AERONAUTICS AND SPACE ACT OF 1958

NASA SCIENTIFIC AND TECHNICAL PUBLICATIONS

TECHNICAL REPORTS: Scientific and technical information considered important, complete, and a lasting contribution to existing knowledge.

TECHNICAL NOTES: Information less broad in scope but nevertheless of importance as a contribution to existing knowledge.

TECHNICAL MEMORANDUMS: Information receiving limited distribution because of preliminary data, security classification, or other reasons.

CONTRACTOR REPORTS: Scientific and technical information generated under a NASA contract or grant and considered an important contribution to existing knowledge.

TECHNICAL TRANSLATIONS: Information published in a foreign language considered to merit NASA distribution in English.

SPECIAL PUBLICATIONS: Information derived from or of value to NASA activities. Publications include conference proceedings, monographs, data compilations, handbooks, sourcebooks, and special bibliographies.

TECHNOLOGY UTILIZATION PUBLICATIONS: Information on technology used by NASA that may be of particular interest in commercial and other non-aerospace applications. Publications include Tech Briefs, Technology Utilization Reports and Notes, and Technology Surveys.

Details on the availability of these publications may be obtained from:

SCIENTIFIC AND TECHNICAL INFORMATION DIVISION

NATIONAL AERONAUTICS AND SPACE ADMINISTRATION

Washington, D.C. 20546